Dynamics of the Inland Penetrating Indian Monsoon Depressions

Sandhyavijayan K[1], Sooraj K.P[1], E. Suhas[2], Pascal Terray[3]

[1]Centre for Climate Change Research, Indian Institute of Tropical Meteorology, Ministry of Earth Sciences, Pune 411008, India
[2] Earth and Climate Science, Indian Institute of Science Education and Research, Pune 411008, India
[3]Sorbonne Universites (UPMC, Univ Paris 06)-CNRS-IRD-MNHN, LOCEAN Laboratory, 4 Place Jussieu, Paris, France

Submitted revised manuscript to Climate Dynamics
October 2025

Corresponding authors address:
Sooraj K. P.
Centre for Climate Change Research, Indian Institute of Tropical Meteorology
Pune 411008, India, https://orcid.org/0000-0003-1246-8922
e-mail: sooraj@tropmet.res.in

Abstract

Despite the decisive role of Bay of Bengal Monsoon Depressions (MDs) in contributing to the Indian summer monsoon mean rainfall, the exact mechanisms and processes contributing to their prolonged residence over the Indian landmass remain still elusive. So, a comprehensive analysis on the factors affecting the inland penetration length of MDs after landfall over the Indian landmass, is presented here using MDs identified from Indian Meteorology Department weather reports over 3 decades (1991-2020). Exploration of large-scale atmospheric circulation features using ERA-5 reanalysis data shed new insights on the processes contributing to the maintenance and sustenance of land penetrating MDs. Notably, all Higher Inland Propagating (HIP) MDs were preceded by Mid-Tropospheric Cyclones (MTCs, with cyclonic circulation in the lower and mid-troposphere) over North-West (NW) India, with this entire region experiencing increased moisture flux convergence, thus facilitating the deep intrusion of MDs into the Indian landmass. In contrast, the Lower Inland Propagating (LIP) MDs experience dry air intrusion from the adjacent desert region, creating unfavorable moisture conditions and leading to their rapid dissipation. Intriguingly, the HIP MDs were further found to cluster with the westward propagating large-scale intraseasonal mode (i.e.,10-20 days). Using the updated GLDAS soil moisture reanalysis, it is further revealed that the precipitation caused by both the MTC and the 10-20 days intraseasonal oscillation mode saturates the land surfaces before the arrival of MDs in the northwestern central Indian region during HIP events. In short, our results provide seminal evidence on the presence of cyclonic vorticity over NW India (with MTC associated circulations), in association with the large-scale westward propagating (10-20 days) mode of variability for creating favorable conditions for the existence of HIP events. Further, the results highlighting the importance of 10-20 days mode and its propensity to cluster with the land penetrating MDs, assume significance in a changing climate, as the subseasonal Indian monsoon rainfall variability is projected to increase in the future.

Key words:

Monsoon Depressions (MDs); High Inland Propagating (HIP) MDs; Low Inland Propagating (LIP) MDs; Mid-Tropospheric Cyclones; Soil Moisture; Intraseasonal Oscillation

1. Introduction

Monsoon Depressions (MDs) are northwestward propagating, rotationally dominant rain-bearing weather systems that bring heavy precipitation to the Indian subcontinent along and near their tracks. MDs contribute to nearly half of the Indian Summer Monsoon (ISM) Rainfall (e.g., Yoon and Chen, 2005; Kishtawal et al., 2013; Cohen and Boos, 2014; Hunt et al., 2016; Patwardhan et al., 2020; Nikumbh et al., 2020, 2021). The large-scale synoptic conditions that favor the MD genesis include upper-tropospheric easterly waves (Sikka, 2006), residual Low-Pressure Systems (LPS), which are cyclonic synoptic scale systems from the South China Sea region migrating westward, (Meera et al., 2019; Vishnupriya et al. 2022), and slow descending cyclonic circulations in the mid-troposphere (Hunt et al., 2016; Patwardhan et al., 2020). Additionally, climatological conditions such as warm sea surface temperatures, low-level cyclonic vorticity, strong vertical wind shear, and abundant moisture extending into the mid-troposphere (Sikka, 1977; Ajayamohan et al., 2010; Hunt et al., 2016) create favorable conditions for the formation and intensification of MDs. Most MDs form over the Bay of Bengal (BoB) and move northwestward along the monsoon trough (Sikka & Gadgil, 1980; Cohen and Boos, 2014).

Given the contribution of MDs to the ISM rainfall and their role in causing catastrophic floods over the Indian subcontinent, a comprehensive understanding on various MD statistics such as frequency of formation, intensity, track, time spent over land, distance traveled after crossing the coastline, and duration are crucial for improving the skill of weather and flood predictions in the region. Many of these factors, especially the track and intensity of MDs, have received significant attention (Krishnamurthy and Ajayamohan 2010; Meera et al., 2019; Patwardhan et al., 2020; Nikumbh et al., 2020, 2021). The MDs are generally expected to rapidly decay over land due to the reduced supply of moisture and energy fluxes from the surface. However, there are cases where MDs penetrate several hundred kilometers into the

103 land and persist for extended periods. Many previous studies have highlighted the critical role
104 of soil moisture in facilitating the deep inland penetration of MDs (Dastoor & Krishnamurthy,
105 1991; Emanuel et al., 2008; Chang et al., 2009; Baisya et al., 2017; Hunt and Turner, 2017).
106 Kishtawal et al. (2013) conducted an observational study on landfalling MDs using predecessor
107 rainfall as an indicator of antecedent soil moisture conditions. They found that the MDs with
108 wetter inland conditions prior to landfall exhibit greater inland penetration compared to those
109 with drier conditions. However, this study has limitations, as it focuses only on locally sourced
110 soil moisture (in-situ moisture from antecedent rainfall).

111 Several modeling studies have been conducted to understand the key differences in MD
112 characteristics over moist and dry land surfaces (Dastoor & Krishnamurthy, 1991; Emanuel et
113 al., 2008; Chang et al., 2009). For example, a regional modeling study by Chang et al. (2009)
114 suggested that a wetter and warmer land surface could lead to more intense landfalling MDs.
115 Recent studies support this hypothesis and emphasize the critical role of soil moisture in
116 enabling deeper inland penetration of MDs, which in turn modulate the distribution and
117 intensity of precipitation (Baisya et al. 2017, Hunt and Turner 2017). Sensitivity experiments
118 by Hunt and Turner (2017) highlighted both local and remote effects of soil moisture on
119 simulating the track and intensity of the MDs. However, it is difficult to generalize their
120 findings, as the simulations were conducted only for a single MD event. Nevertheless, these
121 studies underline the important link between soil moisture and the longevity of MDs. Soil
122 moisture influences the surface energy balance, significantly affecting the water vapor
123 availability, atmospheric stability, and circulation, which, in turn, may modulate the track and
124 intensity of MDs.

125 While acknowledging the importance of soil moisture in modulating the characteristics
126 of MDs, it is crucial to understand the underlying mechanisms that cause soil moisture
127 variations in the first place. Despite modeling studies focusing on the impact of soil moisture

on MDs, there has been little phenomenological exploration of the fundamental mechanisms that sustain and maintain MDs over land. Furthermore, it has yet to be demonstrated that land penetrating MDs are not occurring by chance and that they explain a significant portion of total MDs. The first step to answer these questions is to characterize the spatial and temporal evolution of deep penetrating MDs and their associated large-scale circulation features. This concept was partially explored by Kishtawal et al. (2013); however, they used rainfall as a proxy for soil moisture, and their analysis was primarily based on datasets available before 2008 and hence not an updated study. In this study, we aim to extend and expand their work by using more reliable data sets and incorporating a larger sample of land penetrating MD events from the recent period.

It should be noted that there are only a few studies (e.g., Kishtawal et al. 2013) that have examined whether any large-scale atmospheric circulation features could potentially influence the growth and maintenance of land penetrating MDs. We consider the Mid-Tropospheric Cyclones (MTCs) as one such potential candidate. MTCs are cyclonic systems characterized by quasi-stationary behavior and typically form during the ISM season in the northeastern Arabian Sea near Gujarat (Mak, 1975; Carr, 1977; Francis & Gadgil, 2006; Choudhury et al., 2018; Kushwaha et al., 2021, 2023). Several observational studies have noted the concurrent occurrence of MTCs in the Arabian Sea and westward propagating LPSs in the Bay of Bengal (BoB). According to these studies, as LPSs move westward from the BoB, MTCs tend to intensify (Miller & Keshavamurthy, 1968; Carr, 1977; Choudhury et al., 2018; Kushwaha et al., 2024). It is possible that the MTCs might help sustain and intensify MDs over land by facilitating moisture transport from the Arabian Sea. Another potential factor that could extend the longevity of MDs over land is the Monsoon Intraseasonal Oscillation (MISO). It has been shown that active monsoon conditions over central India increase the likelihood of MD genesis through clustering of synoptic activity (e.g., Yasunari, 1981, Goswami et al., 2003;

Wang 2006; Goswami et al., 2010; Krishnamurthy and Ajayamohan 2010; Suhas et al., 2012; Meera et al., 2019). These active conditions are driven by two modes of subseasonal variability: the northward-propagating 30-60 days oscillations and the westward-propagating 10-20 days quasi-biweekly oscillations (e.g., Goswami et al., 2003; Wang 2006; Goswami et al., 2010; Suhas et al., 2012). However, the relative importance and contribution of these modes in modulating the deep penetration of MDs over land remain unclear.

The unresolved questions on the deep penetration of MDs over land and the main objectives of the study are summarized as follows. What are the large-scale environmental conditions over India and neighboring regions that influence the mechanisms responsible for the inland penetration of BoB MDs? Is there any possible linkage between the sustenance of MDs over the Indian landmass and large-scale MISO modes? With these queries in mind, this study undertakes a phenomenological and process-based approach to understand the physical mechanisms associated with the maintenance and sustenance of MDs over land interiors using diagnostic analysis of observational and reanalysis data sets.

Section 2 outlines the data sets used and the methodology adopted. Section 3 elucidates the observed results and discussions. Finally, Section 4 succinctly summarizes the main conclusions.

2. Data and Methodology

The MD events occurred between June and September during the period from 1991 to 2020 are identified based on the weather reports (https://metnet.imd.gov.in/imdmausam/) prepared by the Indian Meteorological Department (IMD). These identified events are verified by comparing them with the monsoon LPS track database of Hunt and Fletcher (2019). The main precipitation data used in this study are 24-hour accumulated rainfall values with a horizontal resolution of 0.25° × 0.25°, obtained from the IMD (Pai et al., 2014). Since the IMD

178 data is exclusively available over the Indian landmass, the Multi-Source Weighted-Ensemble
179 Precipitation (MSWEP) dataset (Beck et al., 2019), which covers the entire South Asian
180 domain, has been employed to examine the 30-60 days northward-propagating and 10-20 days
181 westward-propagating subseasonal modes. MSWEP data with a spatial resolution of 0.25° ×
182 0.25° are created by combining precipitation information from various platforms, including
183 rain gauges, satellites, and reanalysis products. For exploring the circulation and moisture
184 variability, we used ERA5 reanalysis (Hersbach et al., 2020), at 0.25° × 0.25° horizontal
185 resolution, both at the surface (daily mean relative vorticity at 850-hPa and mean sea level
186 pressure) and at multiple standard pressure levels (daily mean horizontal winds and specific
187 humidity). Hourly Vertical Integral of Divergence of Moisture Flux (VIDMF) data obtained
188 from ERA5 reanalysis is also used for analyzing the link between large-scale circulation and
189 moistening. All these ERA5 variables are analyzed for the common time period of 1991-2020.
190 Daily soil moisture data with a 0.25° × 0.25° horizontal resolution for the period from 1991 to
191 2020 are obtained from the Global Land Data Assimilation System (GLDAS). The GLDAS-
192 2.0 (Rodell et al., 2004) dataset is used for the period 1991-2014, while GLDAS-2.2 (Li et al.,
193 2019) is used for the period 2015-2020. The daily anomalies are estimated by subtracting the
194 daily climatology from the raw data. The subseasonal variability in circulation and precipitation
195 fields is obtained by applying a Butterworth band-pass filter (Butterworth, 1930) on their
196 respective daily anomalies for the two frequency MISO bands. The statistical significance of
197 the composite fields is tested based on a two-tailed Student's *t-test* (Storch and Zwiers, 2002).
198 In this study, we focus exclusively on MD events originating over the BoB, which,
199 after crossing the eastern coastline of the Indian subcontinent, moved in a west-northwestward
200 direction, penetrating into the Indian landmass. During the analysis period, 52 cases of such
201 MD events were identified. Figure 1 shows a composite of precipitation anomalies, constructed
202 using the days after the MD event made landfall, highlighting the distribution of precipitation

over the central Indian region (i.e., secondary rainfall maximum over central India as indicated in Fig 1) which is also equally important, compared to the rainfall maximum in the coastal regions, in causing large-scale floods. It is important to note that many studies attribute the passage of MDs as the main factor that responsible for extreme rainfall events in the central Indian region (e.g., Krishnamurthy et al., 2009; Ajayamohan et al., 2010; Dash et al., 2011; Vittal et al., 2013; Bisht et al., 2018, Nikumbh et al., 2020, 2021). However, the contribution of deep land penetrating MD events to extreme rainfall in the region has yet to be fully accounted for. To explore the characteristics of the deep land penetrating MD events and understand the underlying physical processes that sustain their extended life over land, the identified MD events are classified based on their inland propagation length (IPL). In other words, the MD events were arranged in descending order based on their IPL after landfall: i.e., from the Higher Inland Propagating (HIP) to Lower Inland Propagating (LIP) MD events. The top eight HIP and bottom eight LIP MD events, so identified, are categorized as HIP and LIP MD events, respectively (see Tables 1 and 2). As the extreme precipitation occurs in the vicinity of the MD propagation path, while selecting the top eight HIP events, it is also ensured to account for their association with daily rainfall extremes. The daily extreme rainfall events are identified using a percent threshold with daily rainfall intensities exceeding the 99^{th} percentile (e.g., Krishnamurthy et al., 2009; Ajayamohan et al., 2010; Dash et al., 2011; Vittal et al., 2013; Bisht et al., 2018) over the region of interest, as marked in Figure 1. Finally, the individual tracks of the HIP and LIP MD events, shown in Figure S1, illustrate their contrasting land intrusion characteristics and the tight clustering of the HIP MD events.

Tables 1 and 2 further show an interesting observation that while the LIP events occurring during the core monsoon months of ISM (July and August) are absent, the preference of HIP events to occur in the peak ISM season is the rule in general. In other words, most of the LIP events occur at the beginning or end of ISM period, which is in contrast with HIP

events. The individual tracks of the HIP and LIP MD events illustrate their contrasting land intrusion characteristics and the tight clustering of the HIP MD events (Figure S1).

3. Intrusion of MDs into the Indian landmass: searching for new linkages

As the HIP MD events cluster in a rather narrow path and constitute a significant fraction of all MD events, it is likely that certain large-scale atmospheric features create a favorable environment for their persistence over land and their observed spatial clustering. To identify the large-scale processes that support HIP MD events, life cycle composites of circulation, relative vorticity, moisture transport and soil moisture have been constructed for HIP MD events and compared with those of LIP MD events. Figures 2 and 3 illustrate the spatial and temporal evolution of circulation and Relative Vorticity (here onwards, ζ) anomalies in the lower and mid-troposphere associated with HIP MD events over the South Asian region. The composites reveal a cyclonic circulation anomaly developing over Northwest (NW) India and the adjacent Arabian Sea in both the lower and mid-troposphere several days prior to landfall. This anomaly first appears in the lower troposphere (Figure 2), then intensifies and extends vertically to the mid-troposphere (i.e., MTC associated circulation, e.g., Raymond and Jiang 1990; Choudhury et al., 2018; Nikumbh et al., 2020; Kushwaha et al., 2021, 2023), reaching maximum strength approximately two days before landfall. As the MDs form over the Bay of Bengal (BoB) and propagate northwestward across the Indian landmass, the cyclonic circulation anomaly over NW India begins to weaken (Figures 2 and 3). In contrast, Figures 4 and 5 showing the circulation and ζ anomalies during LIP MD events, exhibit only a weak cyclonic circulation anomaly in the lower and mid-troposphere over NW India prior to landfall. Furthermore, anticyclonic anomalies are observed over this region immediately following landfall. The strength of LIP MD events diminishes quickly as they move toward the Himalayan foothills after landfall. An interesting observation from the figures 2 and 4 is that the low-level circulation is very strong over peninsular India for the HIP events,

254 while it is weaker for LIP events. Hence, shear vorticity of the low-level jet is also conducive
255 in the formation of HIP MDs in contrast to LIPs.

256 Figures 6 and 7 present the life cycle composites of vertically integrated moisture
257 transport from the surface (1000-hPa) to the mid-troposphere (400-hPa) for HIP and LIP MD
258 events, respectively. Figure S2 additionally quantifies the results, as area averaged over the
259 region of interest (20°-25°N and 72°-78°E). For further illustration, the time-longitude
260 distribution (Figure S3) of VIDMF anomaly fields is also prepared. These composites reveal a
261 marked contrast in the spatial and temporal distribution of moisture fluxes between the two
262 types of events. During HIP MD events, before Day 0, widespread moisture flux occurs over
263 the Indian subcontinent, including the Arabian Sea and BoB (see Fig. 6). In particular, the
264 central India experiences stronger and more widespread moisture transport from Arabian Sea
265 (see Fig S2). During the same time period (i.e., Day -2), one can also see strong moisture
266 convergence (Figure S3a, as revealed through negative values of VIDMF) over the northeastern
267 Arabian Sea, and the adjoining NW Indian region for HIP events, thus further signifying the
268 pre-existing cyclonic circulation over NW India well ahead of MDs. In contrast, the LIP MD
269 events exhibit weaker and more localized moisture transport, mainly confined to the northern
270 BoB (Figure 7). Again, for the LIP events, even though there was a slight convergence of
271 moisture over 70°-75°E (Figure S3b), the sign has become opposite (positive VIDMF anomaly)
272 from Day -2 onwards, indicating moisture divergence. In accordance with this, the moisture
273 transport is very weak (Figure 7), with negative anomalies dominating central and northern
274 India, indicating less favorable conditions for convection before the MD's landfall, which may
275 hinder the westward propagation of MDs with low IPL. This is further exemplified in Figure
276 S2, with the LIP MDs exhibiting weak moisture transport compared to HIP on all days. There
277 is a steady drop in moisture transport as the time progress, which could be possibly due to
278 large-scale divergence as stated above. After the landfall, the values even become more

279 negative. Thus, the distribution of moisture fluxes during HIP MD events suggests that active
280 monsoon phases are likely a major factor contributing to the widespread in moisture fluxes.
281 The observed clustering of monsoon LPSs during periods of active monsoon (as highlighted in
282 Introduction) over the central Indian region further supports this hypothesis (e.g., Goswami et
283 al., 2003; Wang 2006).

284 Given that the soil moisture is known to influence the MD characteristics, the spatial
285 and temporal evolution of soil moisture during HIP and LIP MD events is also analyzed (Figure
286 8). This will also contextualize the strong linkage between large-scale moisture transport and
287 soil moisture variability over the Indian landmass. However, soil moisture is a highly localized
288 parameter, and any influence it exerts on MDs is likely limited to the regional scale. To account
289 for differing MD trajectories, composites are created using an MD-centered coordinate system,
290 where the MD location is defined as the origin, and "Lag-0" represents two days after landfall
291 of MD events. Figure 8 (see the figure caption for the methodology followed) illustrates the
292 difference in soil moisture between HIP and LIP MD events, highlighting significant positive
293 soil moisture anomalies during HIP MD events, particularly to the northwest of the MD center.
294 This finding supports the observations of Kishtawal et al. (2013). However, a key distinction
295 in our study is the use of actual soil moisture data, which captures both local (in-situ)
296 precipitation and moisture transported from remote sources such as the Arabian Sea and BoB.
297 In contrast, Kishtawal et al. (2013) relied on antecedent rainfall as a proxy for ground wetness,
298 which only accounts for in-situ moisture.

299 MISO is another large-scale factor that may provide a conducive environment for the
300 occurrence of HIP MD events. The observed clustering of LPS events during active rainfall
301 episodes (Goswami et al., 2010; Suhas et al., 2012; Meera et al., 2019), along with the similarity
302 in spatial rainfall distribution during active rainfall spells and HIP MD events, suggest a
303 supportive role of MISOs in facilitating HIP MD events. However, previous studies have not

clearly established whether both MISO modes (30-60 days mode and 10-20 days mode, e.g., Goswami et al., 2003; Wang 2006) are equally influential in modulating HIP MD events, or one mode plays a more dominant role. A recent study by Karmaker et al. (2021) examined the influence of northward propagating MISOs on the genesis and amplification of MDs. Although they found an association between the intensification of MDs and MISOs, they did not find a significant relationship between the phases of MISOs and MDs. This observation casts doubt on the role of the 30–60 day mode in clustering MD events during the active phase of the ISM and its subsequent role in leading to HIP MD events. To differentiate the contribution of the two MISO modes, we analyze rainfall characteristics associated with both MISO modes during HIP and LIP MD events. Since westward and northward propagating rainfall anomalies are unique features of the two MISO modes, we examine time-longitude (see Fig 9a,c) and time-latitude (see Fig 9b,d) distributions of rainfall anomalies during HIP and LIP MD events, to assess the roles of the MISOs. Figure 9 a,c reveals a marked difference in the 10-20 days MISO rainfall anomalies between HIP and LIP MD events. While the HIP MD events show the presence of a coherent and strong westward propagation of rainfall anomalies (a typical signature of the 10-20 days MISO mode, see Fig 9a), it is conspicuously absent during LIP MD events (see Fig 9c). This contrast underscores the critical role of 10-20 days MISO mode in promoting the HIP MD events. In contrast, rainfall anomalies associated with the 30-60 days MISO mode peak a few days prior to MD rainfall and remain confined south of 20°N during HIP events (Figure 9 b). In other words, latitudinal variation of 30-60 days mode is not prominent, which implies a relatively less influence of this lower frequency mode on synoptic scale MDs. Furthermore, spatial variance analysis of rainfall anomalies for both MISO modes carried out for HIP and LIP MD event days demonstrates the dominant influence of 10-20 days MISO mode during HIP MD events (Fig 10, compare 10a and 10b). It suggests a limited role of the 30-60 days MISO mode in supporting HIP MD events. Figures 11-12 show the lower

and mid-tropospheric circulation anomalies, associated with the 10-20 days MISO mode during various stages of HIP and LIP MD events. The presence of a coherent pair of off-equatorial cyclonic and anticyclonic circulation anomalies, and their westward propagation from west Pacific to central Indian region during HIP MD events (Fig 11) is remarkable, which may further reinforce the pivotal role of the 10-20 days MISO mode during HIP MDs. Because the horizontal scale of the 10–20-day mode is larger than that of MDs (Chatterjee and Goswami, 2004), its occurrence prior to MD formation—contrary to the widely held belief that the 30–60-day mode is dominant—helps establish a favorable environment for MD amplification and enhanced inland penetration, through processes such as land surface saturation from precipitation and moisture advection into the core region of the MD. However, the possible intriguing role of the west Pacific circulation in supporting the westward propagating (10-20 days) mode during HIP events, needs further detailed explorations in the future.

4. Summary and perspectives

This study examines the dynamics of inland penetrating MDs to the Indian subcontinent during ISM period, considering their potential to produce extreme rainfall events and catastrophic flood conditions with tremendous effects (Kishtawal et al., 2013). The goal is to bring new insights on the processes and mechanisms contributing to the maintenance and sustenance of inland penetrating MDs.

Intriguingly, all the HIP MDs exhibit anomalous cyclonic vorticity signatures in the lower to mid-troposphere over NW India prior to its landfall (Figs. 2-3) which is conspicuously absent in the LIP cases (Figs. 4-5). This does not seem to be a coincidence as we inferred that there is a dynamic linkage between the pre-occurring large-scale cyclonic circulation over NW Indian landmass and BoB MD. It is shown that these anomalous circulation features increase the transport of moist Arabian Sea air to the Indian subcontinent (Fig 6 and Fig. S2), thus acting

as a source of moisture content for the atmospheric column over central Indian landmass. Subsequently, an MD reaching central India might be exposed to abundant water vapor content to sustain the MD over landmass and thus allowing them to intrude further westward (i.e., longer IPL). In contrast, the LIP MDs showed a diverging center of moisture flux centered over NW India due to the anticyclonic circulation patterns (Fig S3), which may cause dry air intrusion from heat low over Rajasthan and neighboring regions (Fig 7 and Fig 8; Krishnamurthi et al., 2010; Parker et al., 2016). This creates unfavorable background moisture conditions for the sustenance of the MD structure, which results in the rapid dissipation of MD thus limiting its progression into the Indian landmass through stabilization of lower-atmosphere (Narayanan et al., 2004; Someshwar Das et al., 2007; Das et al., 2021; Singh & Sandeep, 2022; Kushwaha et al. 2024). The contrast in the northwestward propagation of HIP and LIP MD events can also be explained using the Potential Vorticity (PV) framework (Boos et al., 2015, 2017). Boos et al. (2015) demonstrated the role of PV advection in the propagation of MD events. During HIP MD events, the abundant supply of moisture over the landmass northwest of the MD location, within a conditionally unstable monsoon environment, leads to stronger convection and greater latent heat release. This enhanced latent heating induces anomalous circulation patterns that, in turn, facilitate more pronounced inland northwestward propagation of MD events (Boos et al., 2017).

It is interesting to note that most of the LIP events occur at the beginning or end of ISM period, while the HIP events show preference to occur during the peak ISM phase (Table 1, and 2). This distinct seasonality in occurrence of LIP and HIP events suggests strong linkage of these events with the annual cycle. So, the dry air intrusion from Rajasthan and surrounding regions as inferred in the context of LIP events and the absence of it in the HIP events, is further consistent with this observation, as recent studies noted the role of dry air intrusions in marking

the seasonal transition of the monsoon (i.e. onset and withdrawal months of the monsoon, see Parker et al., 2016; Deoras et al 2024).

Further examination of the association of sub-seasonal modes of variability with MDs revealed a strong linkage between HIP MDs and a westward propagating 10-20 days mode, with only a limited role from the northward propagating 30-60 days mode (see Figs 9 and 10). Thus, the preference of HIP MDs to concur with the large-scale 10-20 days mode, as highlighted here, brings a new perspective as the prevailing wisdom advocates that the dominant intraseasonal variability (i.e., 30-60 days mode) tends to cluster MD activity, as stated in Introduction. It is also revealed that HIP MDs had higher soil wetness, due to the precipitation primarily caused by both MTCs and 10-20 days MISO mode (but with a secondary contribution from the 30-60 days mode, see Fig. 8), over the area ahead of the MD compared to LIP MDs, thus allowing HIP MDs to penetrate deeper into the land before dissipation. This is in line with prior investigation using antecedent rainfall data (Kishtawal et al., 2013). It is further inferred that the atmospheric circulation patterns associated with the 10-20 days mode facilitate the northwestward movement of HIP MD events (see Fig 11). In LIP events, where the 10-20 days mode and associated circulations are absent, the MDs take climatological path and end near Eastern Himalayan foothills (see Fig 12).

In brief, our results reveal the influential role of MTC and 10-20 days MISO mode in facilitating the sustenance and westward propagation of HIP MD events. Thus, the analysis reveals that the occurrence of MTC prior to MD landfall is very critical for HIP MD events (see Figs. 2-3). The cyclonic circulation associated with the MTC not only helps in sustaining the cyclonic circulations but also strengthens and extends the longevity of the MD events by bringing moisture laden air from the Arabian sea (Figs. 6 and 7). Clear contrasts observed in vertically integrated moisture transport for HIP and LIP events further support this inference (Fig S2). Additionally, precipitation caused by both MTCs and 10-20 days MISO mode

403 saturates the land surfaces ahead of MDs arrival over the NW central Indian region (see Figs.
404 8 and 9). The higher soil moisture content ahead of MDs helps in sustaining the MDs over the
405 landmass (see Fig 8). For example, higher soil moisture increases the evaporation and provides
406 additional moisture to the atmosphere, lowering the sensible heat flux and hence cooling the
407 surface (Seneviratne et al. 2010). This sets up a wet cool boundary layer, which in turn, acts to
408 vertically extend the warm core of the MD and increase the convectively available potential
409 energy around the MD (Hunt and Turner, 2017). This result suggests the well-known warm
410 over cold structure of MDs (Praveen et al., 2015) with a steeper vertical temperature gradient
411 which is an indication of strengthened MD (Hunt et al, 2016). The latent heat released during
412 condensation strengthens the MD by providing the necessary energy to sustain its circulation
413 (Baisya et al., 2017). Finally, according to the moisture-vortex instability theory (Adames and
414 Ming, 2018), enhanced moisture content ahead of the MD by creating a positive moisture
415 gradient facilitates a favorable environment for convection and the development of atmospheric
416 disturbances, thus supporting the maintenance and propagation of HIP MDs.

417 The results from this study have larger implications. Firstly, it suggests a possibility
418 that by closely monitoring these antecedent circulation features originating in the Gujarat or
419 NW Indian region, we might improve the anticipation of intense MDs that could travel farther
420 west-northwestward across the Indian landmass. Our study assumes further importance, as
421 recent studies showed an increasing trend in the extreme daily rainfall intensities over the
422 regions of our interest (Ajayamohan et al., 2010; You and Ting 2021), which calls for careful
423 monitoring of MTCs and other cyclonic circulations over NW India and BoB MDs to better
424 anticipate the flood-producing daily rainfall extremes.

425 Finally, as per Menon et al. (2013), the sub-seasonal ISM rainfall variability is
426 increasing with global mean temperature under an unmitigated climate change scenario. So,
427 the current results highlighting the importance of 10-20 days mode and its tendency to cluster

with the land penetrating MDs may have larger implications in a global warming scenario. Moreover, Sandeep et al. (2018) showed a shift in the MDs to the Indian landmass in the future warming scenario. In this context, as part of future research work, we may explore whether the land-falling MDs exhibit analogous increasing trends using CMIP6 future projections.

Acknowledgments

We sincerely thank the Director, Indian Institute of Tropical Meteorology (IITM, India) and the Project Director, Centre for Climate Change Research (CCCR at IITM) for all the support during the research study. Sandhya Vijayan K and Sooraj K P are funded by the CCCR and IITM, which are fully funded by the Ministry of Earth Sciences, Government of India. Pascal Terray is funded by Institut de Recherche pour le Développement (IRD, France).

Funding

The authors have no funding reference to declare.

Data Availability

All the observational datasets used in this study are publicly available, and the reanalysis datasets used for this study are also available in public. The analysis was carried out utilizing open-source software tools such as the Climate Data Operators and Python (https://www.python.org/) for the computations and visualizations.

Conflict of interest

The authors have not disclosed any competing interests.

Author Contributions

Sandhya Vijayan K (SVK) conducted the analysis, formulated methodology, handled software and visualization tools, analysed the results, and wrote the original manuscript. SKP (Sooraj K P), SE (Suhas E) and TP (Terray Pascal) wrote the original draft, reviewed and edited the manuscript.

References

Adames, Á. F. and Y. Ming, (2018): Moisture and moist static energy budgets of South Asian monsoon depressions in GFDL AM4.0, J. Atmos. Sci., 75, 2107–2123

Ajayamohan R. S., Merryfield W. J., Kharin V. V. (2010). Increasing trend of synoptic activity and its relationship with extreme rain events over central India, Journal of Climate, 23, 1004–1013

Baisya, H., Pattnaik, S., & Rajesh, P. V. (2017). Land surface-precipitation feedback analysis for a landfalling monsoon depression in the Indian region. Journal of Advances in Modeling Earth Systems, 9(1), 712-726.

Beck H. E, Wood E. F, Pan M., Fisher C. K., Miralles D. G., van Dijk A. I., McVicar TR, Adler RF (2019) MSWEP V2 global 3-hourly 0.1deg precipitation: methodology and quantitative assessment. Bull Am Meteorol Soc pp BAMS–D–17–0138.1, https://doi.org/10.1175/BAMS-D-17-0138.1

Bisht, D. S., Chatterjee, C., Raghuwanshi, N. S., & Sridhar, V. (2018). Spatio-temporal trends of rainfall across Indian river basins. Theoretical and Applied Climatology, 132(1–2), 419–436. https://doi.org/10.1007/s00704-017-2095-8

Boos, W.R., Hurley, J.V. and Murthy, V.S. (2015), Adiabatic westward drift of Indian monsoon depressions. Q.J.R. Meteorol. Soc., 141: 1035-1048. https://doi.org/10.1002/qj.2454.

Boos WR, Mapes BE, Murthy VS (2017) Potential vorticity structure and propagation mechanism of Indian monsoon depressions. The Global Monsoon System: Research and Forecast, World Scientific, 187–199.

Butterworth S, “On the Theory of Filter Amplifiers,” Experimental Wireless and the Wireless Engineer, Vol. 7, 1930, pp. 536-541.

Carr, F. H. (1977). Mid-tropospheric cyclones of the summer monsoon. Pure and applied geophysics, p. 115, 1383–1412.

Cohen, N. Y., and W. R. Boos. (2014). Has the number of Indian summer monsoon depressions decreased over the last 30 years? Geophysical Research Letters, pp. 41, 7846–7853

Chang, H. I., Niyogi, D., Kumar, A., Kishtawal, C. M., Dudhia, J., Chen, F., ... & Shepherd, M. (2009) Possible relation between land surface feedback and the post-landfall structure of monsoon depressions. Geophysical Research Letters, 36(15).

Choudhury, A. D., Krishnan, R., Ramarao, M. V. S., Vellore, R., Singh, M., & Mapes, B. (2018). A phenomenological paradigm for mid-tropospheric cyclogenesis in the Indian summer monsoon. Journal of the Atmospheric Sciences, 75(9), 2931–2954.

Das, Someshwar, R. Ashrit, Mitchell W. Moncrieff, M. Dasgupta, J. Dudhia, C. Liu and S. R. Kalsi, (2007) Simulation of Intense Organized Convective Precipitation Observed during the Arabian Sea Monsoon Experiment (ARMEX), J. Geophys. Res., 112, D20117, doi:10.1029/2006JD007627.

Das, S.K., Thatte, T., Uma, K.N., Krishna, U.V.M. & Saha, S.K. (2021) Characteristics of temperature inversion from radiosonde measurements in the western ghats region. Atmospheric Research, 250, 105391. Available from: https://doi.org/10.1016/j.atmosres.2020.105391

Dash, S. K., Nair, A. A., Kulkarni, M. A., & Mohanty, U. C. (2011). Characteristic changes in the long and short spells of different rain intensities in India. Theoretical and Applied Climatology, 105(3), 563–570. https://doi.org/10.1007/s00704-011-0416-x

Dastoor, A., & Krishnamurti, T. N. (1991). The landfall and structure of a tropical cyclone: The sensitivity of model predictions to soil moisture parameterizations. Boundary-layer meteorology, 55(4), 345–380.

514 Deoras A, Andrew G. Turner, Ambrogio Volonté, Arathy Menon (2024) The role of
515 midlatitude dry air during the withdrawal of the Indian summer monsoon. Quarterly Journal of
516 the Royal Meteorological Society, 150(682), 3701-3721. https://doi.org/10.1002/qj.4859
517 Emanuel, K., J. Callaghan, and P. Otto (2008), A hypothesis for the re-development of warm-
518 core cyclones over northern Australia, Mon. Weather Rev., 136, 3863–3872,
519 doi:10.1175/2008MWR2409.1
520
521 Francis, P. A., & Gadgil, S. (2006). Intense rainfall events over the west coast of India.
522 Meteorology and Atmospheric Physics, 94(1-4), 27-42
523 Goswami, B. B., P. Mukhopadhyay, R. Mahanta, and B. N. Goswami (2010), Multiscale
524 interaction with topography and extreme rainfall events in the northeast Indian region, J.
525 Geophys. Res., 115, D12114, doi:10.1029/2009JD012275.
526 Goswami, B. N., R. S. Ajayamohan, P. K. Xavier, and D. Sengupta (2003) Clustering of
527 synoptic activity by Indian summer monsoon intraseasonal oscillations, Geophys. Res. Lett.,
528 30(8), 1431, doi:10.1029/2002GL016734
529 Hersbach, H., Bell, B., Berrisford, P., Hirahara, S., Horányi, A., Muñoz-Sabater, J., ... &
530 Thépaut, J. N. (2020). The ERA5 global reanalysis. Quarterly Journal of the Royal
531 Meteorological Society, 146(730), 1999-2049
532 Hunt, K.M.R. and Fletcher, J.K. (2019) The relationship between Indian monsoon rainfall and
533 low-pressure systems. Clim Dyn 53, 1859–1871. https://doi.org/10.1007/s00382-019-04744-x
534 Hunt, K., Turner, A. G., Inness, P. M., Parker, D. E., Levine, R. C. (2016). On the structure
535 and dynamics of Indian monsoon depressions. Monthly Weather Review, pp. 144, 3391–3416.
536 Hunt, K. M., & Turner, A. G. (2017). The effect of soil moisture perturbations on Indian
537 monsoon depressions in a numerical weather prediction model. Journal of Climate, 30(21),
538 8811-8823.

539 Karmakar, N., Boos, W. R., & Misra,V. (2021). Influence of intraseasonal variability on the
540 development of monsoon depressions. Geophysical Research Letters, 48, e2020GL090425.
541 https://doi.org/10.1029/2020GL090425.
542 Kishtawal, C. M., Niyogi, D., Rajagopalan, B., Rajeevan, M., Jaiswal, N., & Mohanty, U. C.
543 (2013). Enhancement of inland penetration of monsoon depressions in the Bay of Bengal due
544 to prestorm ground wetness. Water resources research, 49(6), 3589-3600
545 Krishnamurthy, C. K. B., Lall, U., & Kwon, H. H. (2009). Changing frequency and intensity
546 of rainfall extremes over India from 1951 to 2003. Journal of Climate, 22(18), 4737–4746.
547 https://doi.org/10.1175/2009JCLI2896.1
548 Krishnamurthy, V. and Ajayamohan, R.S. (2010) Composite structure of monsoon low-
549 pressure systems and its relation to Indian rainfall. Journal of Climate, 23, 4285–4305
550 Krishnamurthi TN, Thomas A, Simon A, Kumar V (2010) Desert air incursions, an overlooked
551 aspect, for the dry spells of the Indian summer monsoon. J Atmos Sci 67(10):3423–3441.
552 https://doi.org/10.1175/2010JAS3440.1
553 Kushwaha, P., Sukhatme, J., & Nanjundiah, R. S. (2021). A Global Tropical Survey of
554 Midtropospheric Cyclones, Monthly Weather Review, 149(8), 2737-2753.
555 Kushwaha, P., Sukhatme, J., & Nanjundiah, R. S. (2023). Classification of mid-tropopsheric
556 cyclones over the Arabian Sea and western India. Quarterly Journal of the Royal
557 Meteorological Society, 149(754), 1572-1592. https://doi.org/10.1002/qj.4466
558 Kushwaha, P., Sukhatme, J., & Nanjundiah, R. S. (2024). Role of Bay of Bengal low-pressure
559 systems in the formation of mid-tropospheric cyclones over the Arabian Sea and western India.
560 Quarterly Journal of the Royal Meteorological Society, 150(762), 2625-2645.
561 https://doi.org/10.1002/qj.4726

562 Li, B., M. Rodell, S. Kumar, H. Beaudoing, A. Getirana, B.F. Zaitchik, et al. (2019) Global
563 GRACE data assimilation for groundwater and drought monitoring: Advances and challenges.
564 Water Resources Research, 55, 7564-7586.
565 Mak, M. K. (1975). The monsoonal mid-tropospheric cyclogenesis. Journal of Atmospheric
566 Sciences, 32(12), 2246-2253.
567 Miller, F. R. and Keshavamurthy, R. N. (1968), Structure of an Arabian Sea summer monsoon
568 system, Meteorological Monograph 1, East-West Center Press, 94
569 Meera, M., Suhas, E., Sandeep, S. (2019) Downstream and in Situ: two Perspectives on the
570 Initiation of Monsoon Low-pressure Systems over the Bay of Bengal, Geophysical Research
571 Letters, 46, 12303-12310
572
573 Menon, A., Levermann, A., & Schewe, J. (2013). Enhanced future variability during India's
574 rainy season. Geophysical Research Letters, 40(12), 3242-3247.
575 https://doi.org/10.1002/grl.50583
576 Narayanan, M.S., Rao, B.M., Shah, S., Prasad, V.S. and Bhat, G.S. (2004) Role of atmospheric
577 stability over the Arabian Sea and the unprecedented failure of monsoon 2002. Current Science,
578 86(7), 938–947.
579 Nikumbh, A.C., Chakraborty, A., Bhat, G., Frierson, D.M. (2020) Large-scale extreme rainfall-
580 producing synoptic systems of the Indian summer monsoon. Geophys. Res. Lett., 47,
581 e2020GL088403
582 Nikumbh, A. C., A. Chakraborty, G. S. Bhat, and D. M. W. Frierson, 2021: Multiscale
583 Interactions between Monsoon Intraseasonal Oscillations and Low Pressure Systems That
584 Produce Heavy Rainfall Events of Different Spatial Extents. J. Climate, 34, 9523–9534,
585 https://doi.org/10.1175/JCLI-D-21-0231.1

586 Pai, D. S., Rajeevan, M., Sreejith, O. P., Mukhopadhyay, B., & Satbha, N. S. (2014).
587 Development of a new high spatial resolution (0.25× 0.25) long period (1901-2010) daily
588 gridded rainfall data set over India and its comparison with existing data sets over the region.
589 Mausam, 65(1), 1-18
590 Parker, D.J., Willetts, P., Birch, C., Turner, A.G., Marsham, J.H., Taylor, C.M., Kolusu, S. and
591 Martin, G.M. (2016), The interaction of moist convection and mid-level dry air in the advance
592 of the onset of the Indian monsoon. Q.J.R. Meteorol. Soc., 142: 2256-2272.
593 https://doi.org/10.1002/qj.2815
594 Patwardhan, S., Sooraj, K.P., Varikoden, H., Vishnu, S., Koteswararao, K., Ramarao, M.V.S.
595 & Pattanaik, D.R. (2020) Synoptic scale systems. In: Krishnan, R., Sanjay, J., Gnanaseelan, C.,
596 Praveen, V., S. Sandeep, and R. S. Ajayamohan, 2015: On the Relationship between Mean
597 Monsoon Precipitation and Low Pressure Systems in Climate Model Simulations. J. Climate,
598 28, 5305-5324, https://doi.org/10.1175/JCLI-D-14-00415.1.
599 Mujumdar, M., Kulkarni, A. and Chakraborty, S. (Eds) Assessment of Climate Change over
600 the Indian Region. Singapore: Springer, pp. 143–154.
601 Raymond, D.J. and Jiang, H. (1990) A theory for long-lived mesoscale convective systems. J.
602 Atmos. Sci. 47, 3067–3077
603 Rodell, M., Houser, P. R., Jambor, U. E. A., Gottschalck, J., Mitchell, K., Meng, C. J., ... &
604 Toll, D. (2004). The global land data assimilation system. Bulletin of the American
605 Meteorological society, 85(3),381-394
606
607 Sandeep, S., R.S. Ajayamohan, W.R. Boos, T.P. Sabin & V. Praveen, Decline and poleward
608 shift in Indian summer monsoon synoptic activity in a warming climate, Proc. Natl. Acad. Sci.
609 U.S.A. 115 (11) 2681-2686, https://doi.org/10.1073/pnas.1709031115 (2018).

610 Seneviratne, S.I, Corti, T., Davin, E.L., Hirschi, M., Jaeger, E.B., Lehner I., Orlowsky, B.,
611 Teuling A.J. (2010) Investigating soil moisture-climate interactions in a changing climate: A
612 review. Earth Sci. Rev. 99, 125–161.
613 Sikka, D. R. (1977) Some aspects of the life history, structure and movement of monsoon
614 depressions, Pure and Applied Geophysics, 115, 1501–1529
615 Sikka, D.R. and Gadgil, S. (1980) On the Maximum Cloud Zone and the ITCZ over Indian,
616 Longitudes during the Southwest Monsoon. Monthly Weather Review, 108, 1840-1853.
617 Sikka, D. R. (2006) A study on the monsoon low pressure systems over the Indian region and
618 their relationship with drought and excess monsoon seasonal rainfall, Center for Ocean-Land-
619 Atmosphere Studies Technical Report, 217, 61
620 Singh, R., Sandeep, S. (2022) Dynamics of dry air intrusion over India during summer
621 monsoon breaks. Clim Dyn 59, 1649–1664. https://doi.org/10.1007/s00382-021-06060-9
622 Storch HV, Zwiers FW (2002) Statistical analysis in climate research. Cambridge University
623 Press, UK, p 494
624 Suhas, E., Neena, J. M., and Goswami, B. N. (2012) Interannual Variability of Indian Summer
625 Monsoon arising from Interactions between Seasonal Mean and Intraseasonal Oscillations, J.
626 Atmos. Sci., 69, 1761–1774, https://doi.org/10.1175/JAS-D-11-0211.1
627
628 Vittal, H., Karmakar, S., & Ghosh, S. (2013). Diametric changes in trends and patterns of
629 extreme rainfall over India from pre-1950 to post-1950. Geophysical Research Letters, 40,
630 3253–3258. https://doi.org/10.1002/grl.50631
631 Vishnupriya S., E. Suhas & S. Sandeep (2022). Extratropical stratospheric air intrusions over
632 the western north Pacific and the genesis of downstream monsoon low-pressure
633 systems, *Geophysical Research Letters*, 49 (23), https://doi.org/10.1029/2022GL100976.
634 Wang, B., 2006: The Asian Monsoon. Springer, 787 pp.

Yasunari, T. (1981) Structure of an Indian Summer Monsoon System with Around 40-Day Period. Journal of Meteorological Society of Japan, 59, 336-354.

Yoon, J.-H., Chen, T. C. (2005) Water vapor Budget of the Indian monsoon depression, Tellus, 57A, 770–782

You, Y., & Ting, M. (2021). Observed trends in the South Asian monsoon low-pressure systems and rainfall extremes since the late 1970s. Geophysical Research Letters, 48, e2021GL092378. https://doi.org/10.1029/2021GL092378

Landfall day	IPL (degree longitude)	Duration (days)	Duration after landfall (days)

20-08-1997	12.5	10	8
25-07-2003	13.6	6	5
30-07-2005	11.7	7	5
02-07-2006	10.7	8	5
03-08-2006	10.2	12	9
05-07-2007	11.5	8	6
20-07-2009	12.1	8	6
07-08-2019	19.6	10	6

658

659 **Table 1:** Details of the MDs (date of landfall of each MDs along with their inland propagation

660 length IPL, in degree longitudes) as categorized under HIP

661

Landfall day	IPL (degree longitude)	Duration (days)	Duration after landfall (days)
22-09-1991	0.6	5	2
17-09-1995	1.9	2	1
26-09-1995	0.9	2	1
27-06-1997	1.4	6	3
28-08-1997	1.9	5	5
27-08-2003	2.2	4	3
20-09-2006	1.0	9	4
22-09-2011	2.0	5	4

662

663 **Table 2:** Details of the MDs under LIP

664

665

666 **Main Figures**

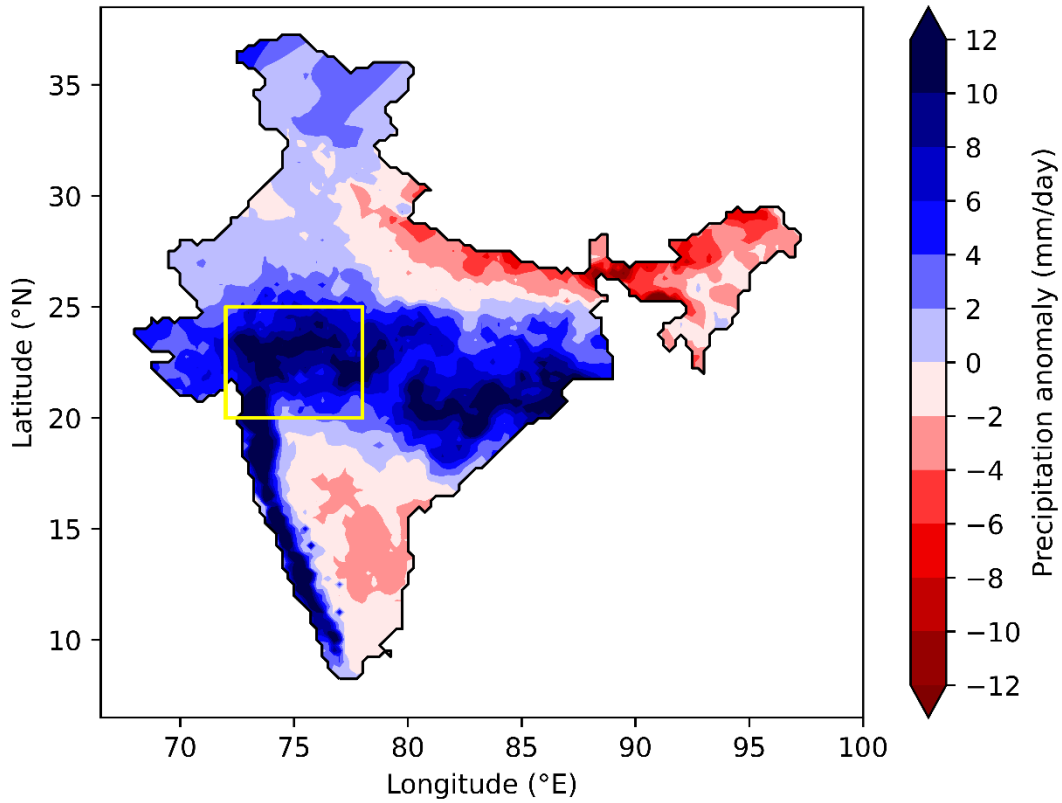
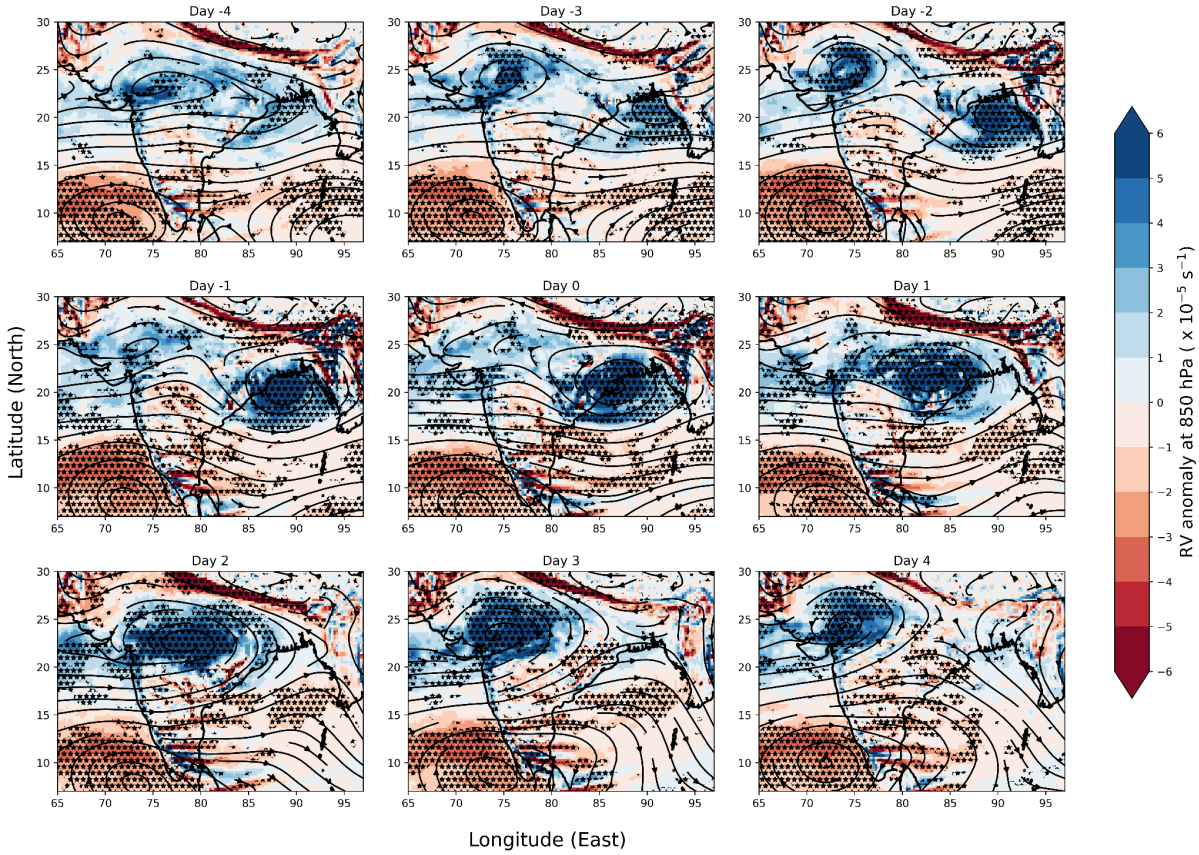


Figure 1: Composite plot for precipitation (mm day-[1]) anomaly for MD days post landfall (a total of 249 days corresponding to 52 MDs). The anomaly is calculated by subtracting daily climatology from the observed data. Selected region is indicated by the yellow box (20°-25°N and 72°-78°E).



675

676 **Figure 2:** Time-lagged (from Day -4 to Day 4) plot of daily ζanomalies (x10^{-5} s^{-1}) along with
677 streamlines at 850 hPa, as composited for the HIP MD events (see Section 2). Day 0 is the
678 landfall day of each MD. In all the panels, the anomalies that are above 90% confidence levels
679 are indicated by asterisk (*).

680

681

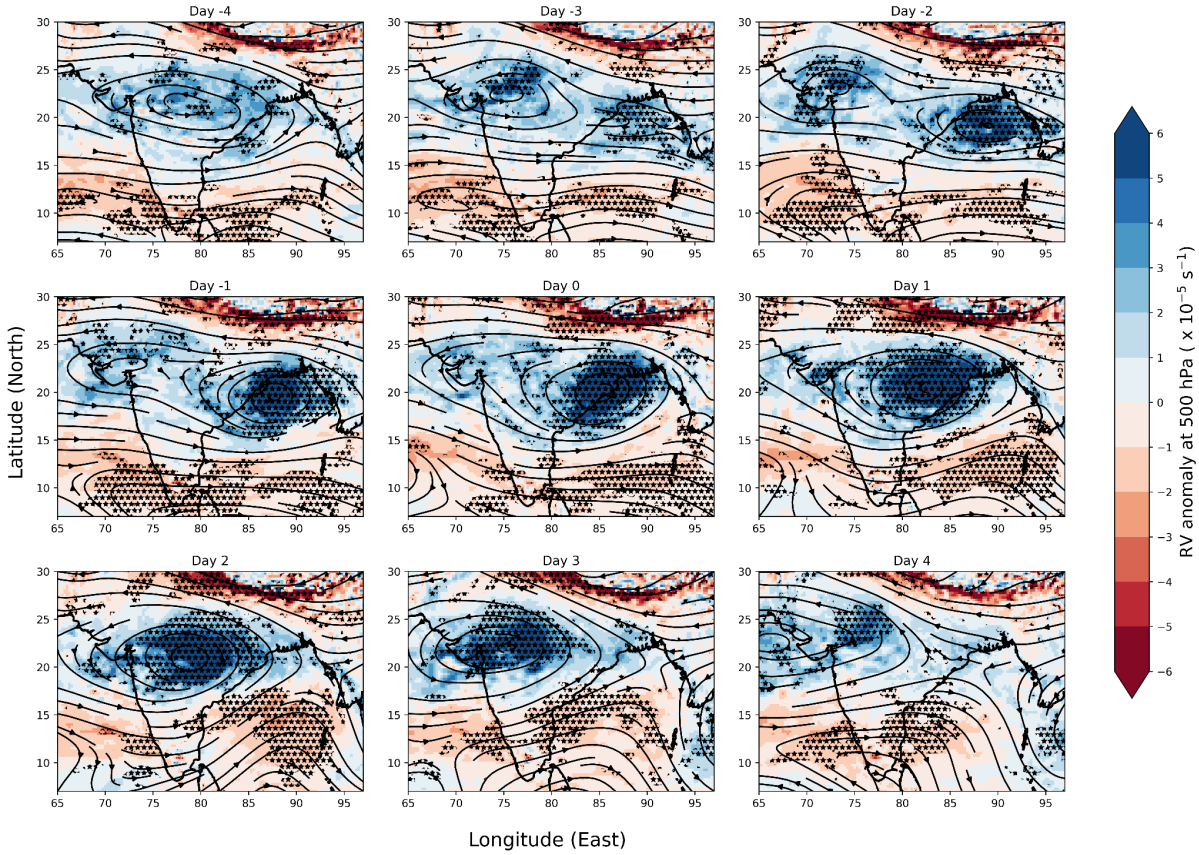
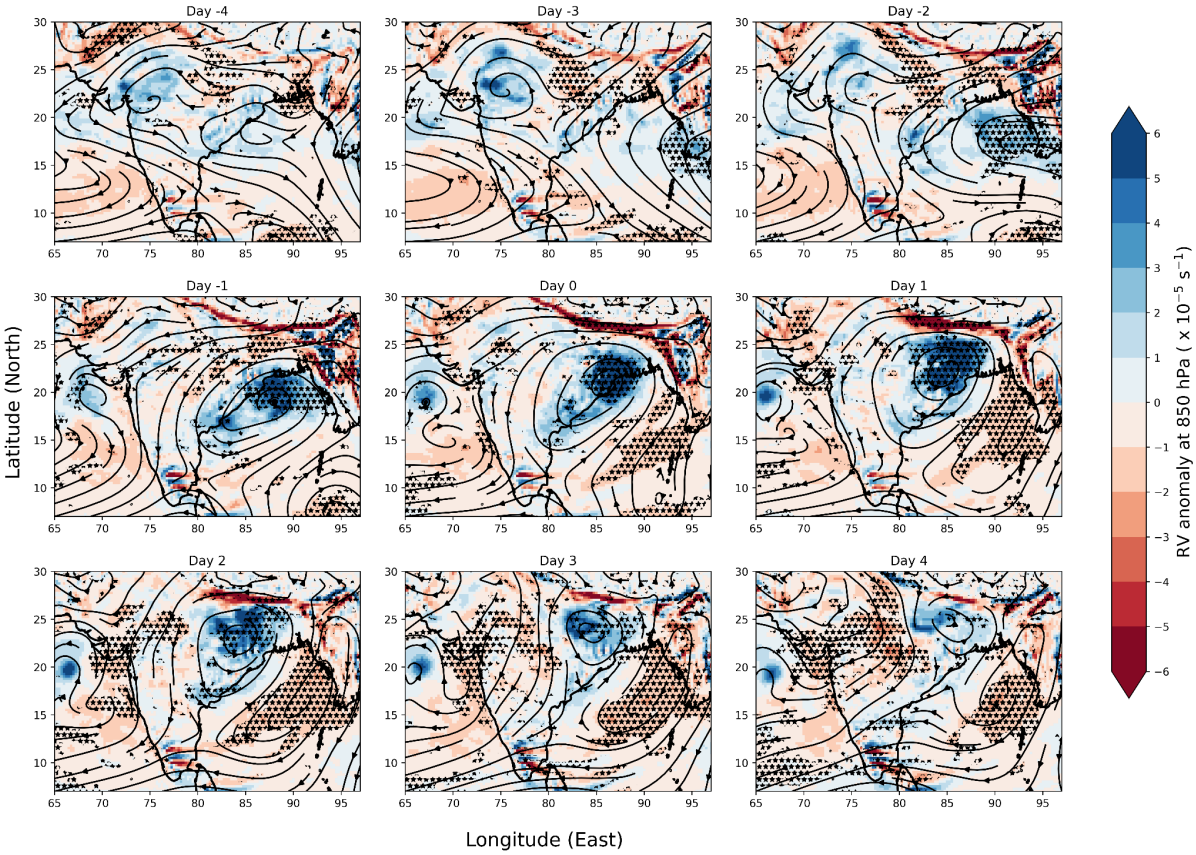


Figure 3: Same as Figure 2, but for the composite plot of HIP MD events at 500 hPa.



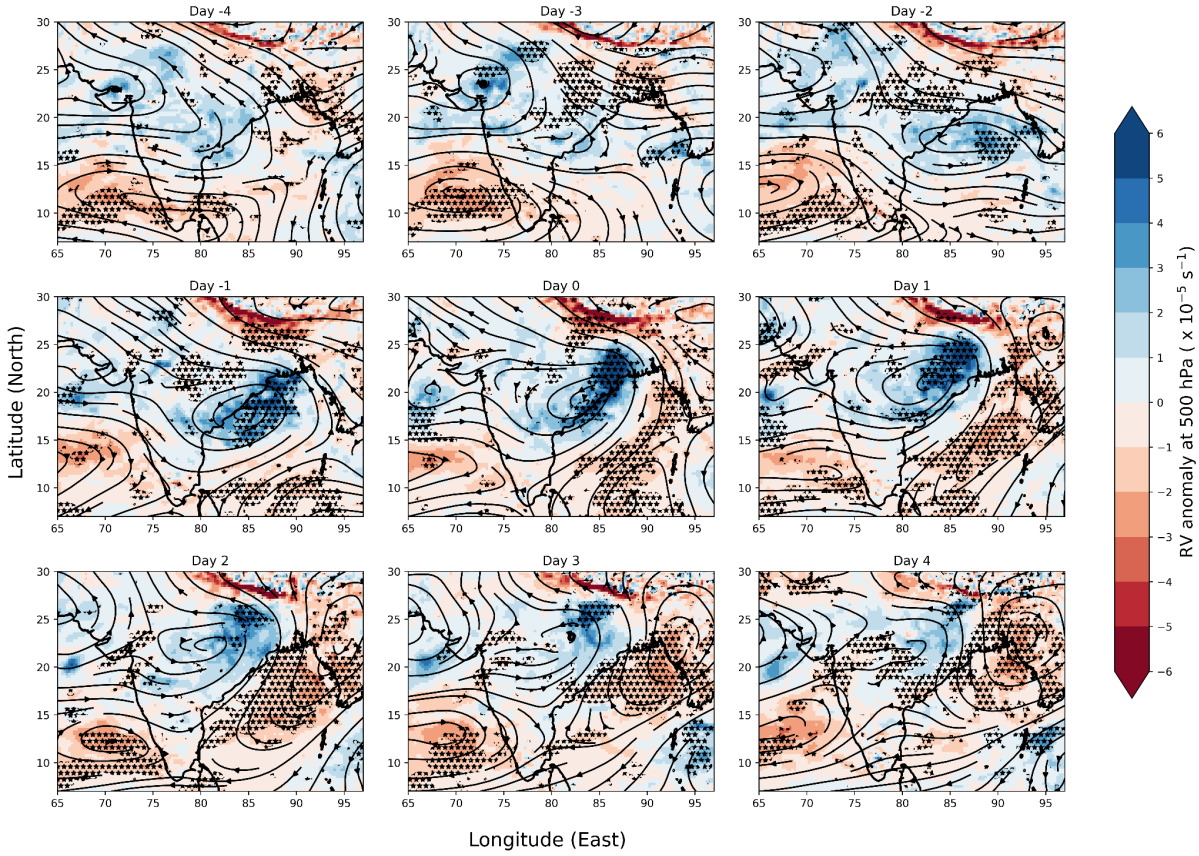
687

688 **Figure 4:** Time-lagged (from Day -4 to Day 4) plot of daily ζanomalies ($x10^{-5}s^{-1}$) along with

689 streamlines at 850 hPa, as composited for the LIP MD events (see Section 2). In all the panels,

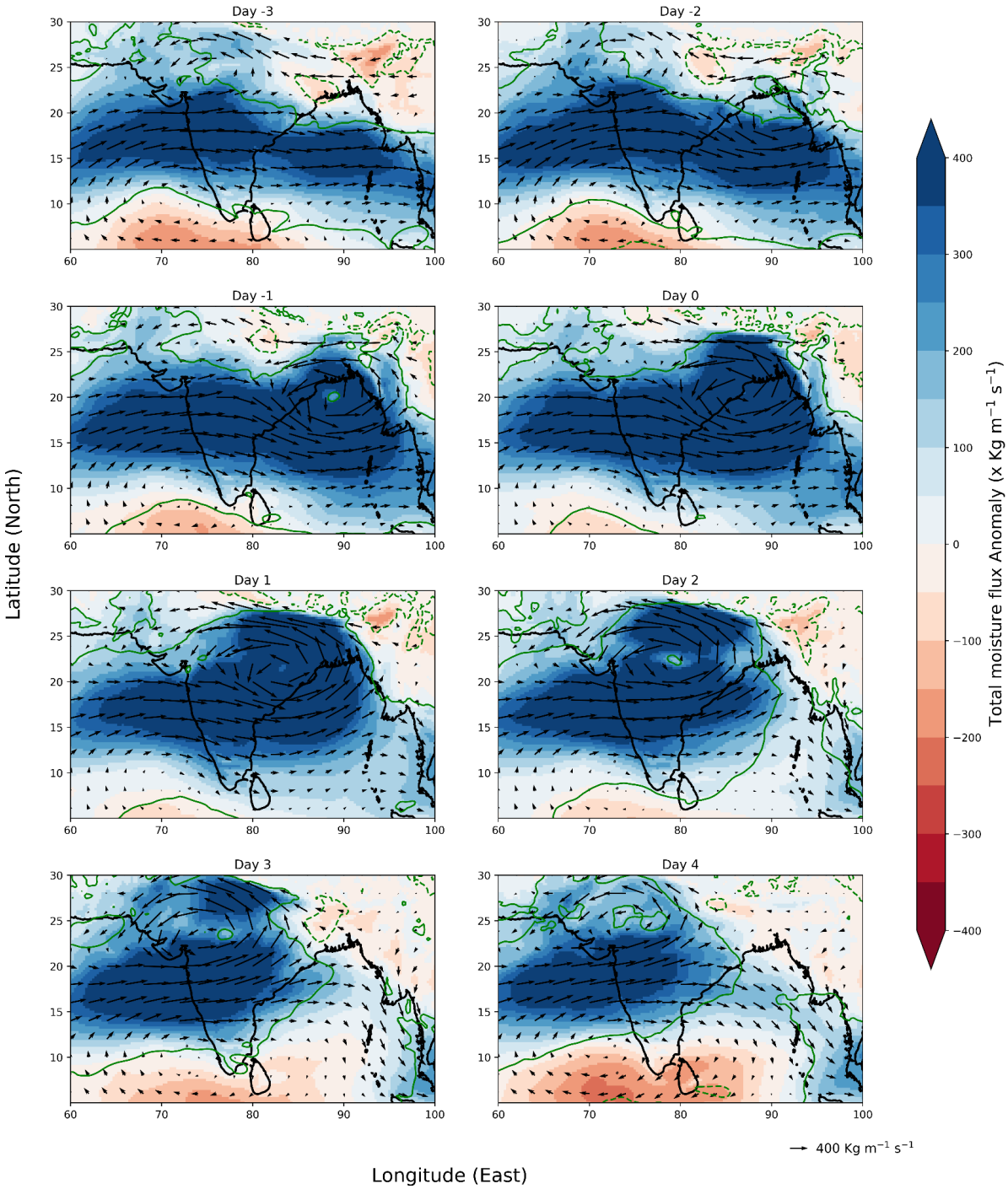
690 the anomalies that are above 90% confidence levels are indicated by asterisk (*).

691



692

693 **Figure 5:** Same as Figure 4, but for the composite plot of LIP MD events at 500 hPa



694

695 **Figure 6:** Time-lagged (from Day -3 to Day 4) composite plot of vertically integrated
696 anomalous moisture transport for HIP MD events. The color shades represent the magnitude
697 of the moisture transport (in Kg m^{-1} s^{-1}), with black vectors indicating the direction of the
698 moisture transport. Vertical integration of moisture transport is performed from 1000hPa to
699 400hPa levels. In all the panels, green contours indicate the anomalies that are above 90%

confidence levels, with solid lines for positive anomalies and dashed lines for negative anomalies.

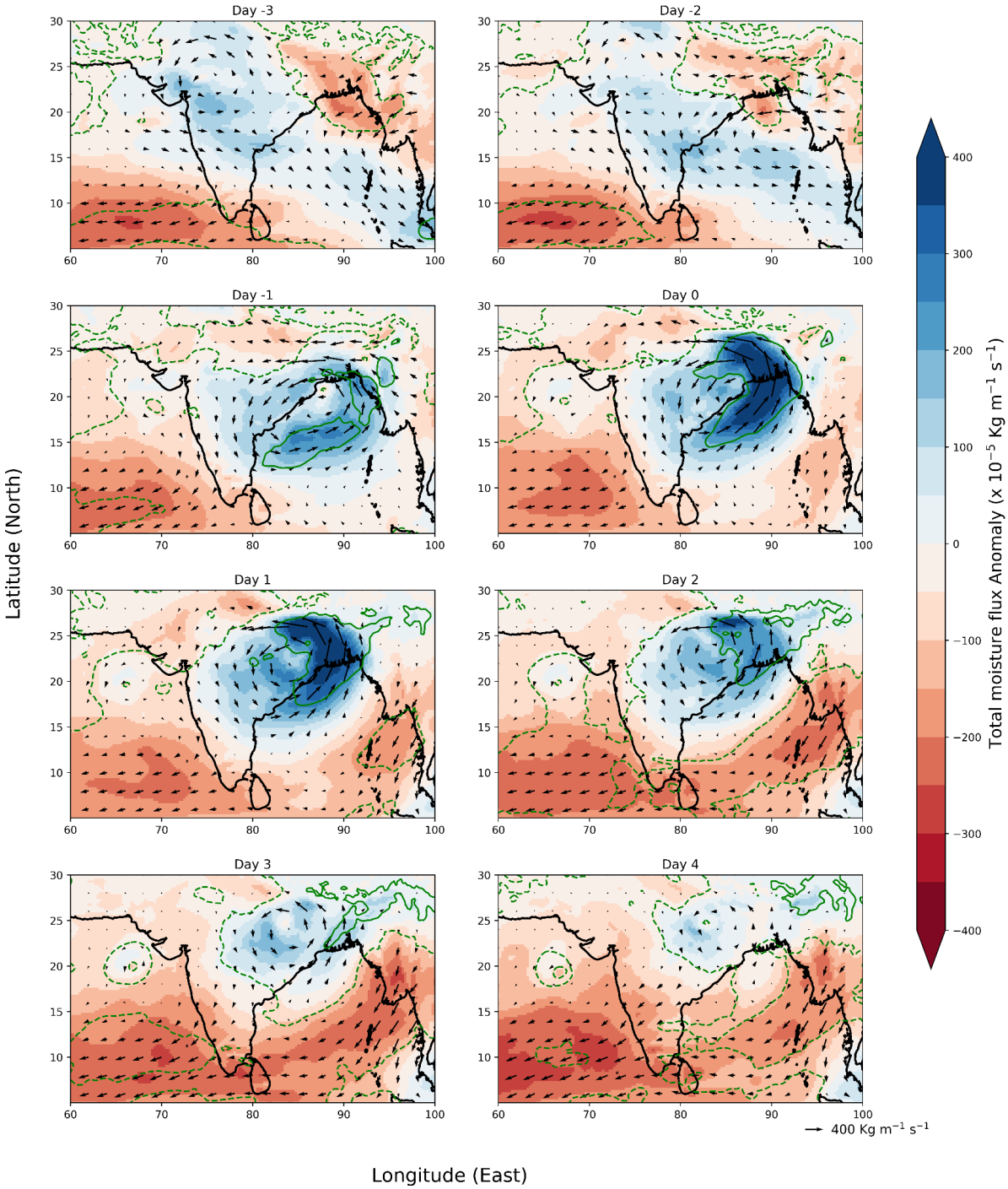


Figure 7: Same as Figure 6, but for the composite plot of LIP MD events from Day -3 to Day 4.

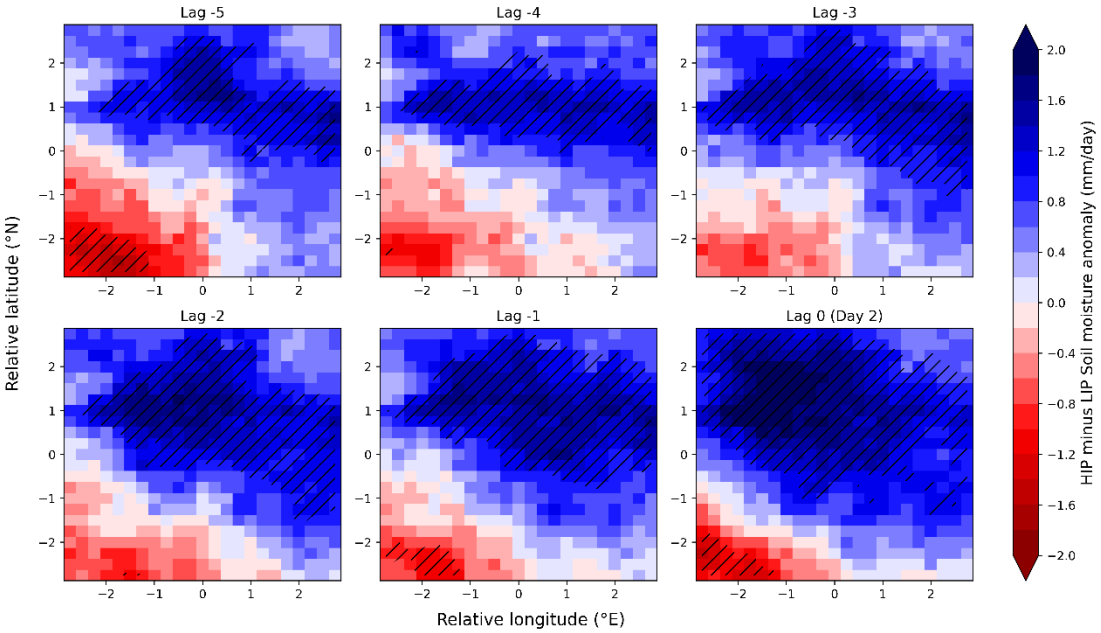


Figure 8: The relative longitude-relative latitude plot of contrast between the HIP and LIP composites for soil moisture content above the Day 2 (i.e., 2 days after landfall) region, from Lag -5 to Lag 0. For Day 2 of each MD, the highest positive ζanomaly at 850 hPa level is identified and assigned as the location of the vortex center of the MD. Then, the soil moisture content above the Day 2 region is determined for the day when the MD is above this region (as designated by Lag 0). This computation is performed for each HIP and LIP MD events and also went backward in time by 1, 2, and 3 days with respect to Lag 0 (as marked by Lag -1, Lag-2, and Lag -3, respectively). The soil moisture information is then centralized to 0° latitude and 0°longitude to create relative longitude - relative latitude composites. The contrast in soil moisture content is depicted by subtracting out the LIP composite from the HIP composite. The hatches represent the regions where the composite difference is statistically significant above 90% confidence level. Units are in mm day^{-1}.

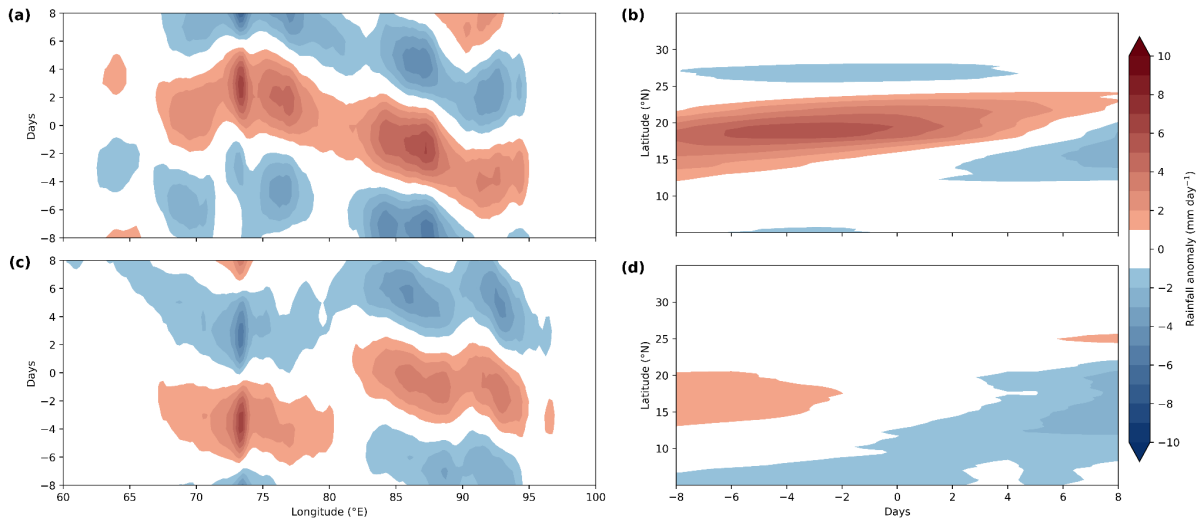


Figure 9: Time-longitude (in a and c) and time-latitude (in b and d) distributions of rainfall anomalies as composited for HIP and LIP MD events, respectively, from Day -8 to Day 8. In (a) and (c), 10-20 days bandpass filtered precipitation anomalies (i.e., latitudinally averaged between 20-25°N) with longitude on the x-axis for HIP and LIP composites, respectively. In (b) and (d), 30-60 days bandpass filtered precipitation anomalies (longitudinally averaged between 70-90°E) with latitude on the y-axis for HIP and LIP composites, respectively. Units are in mm day^{-1}.

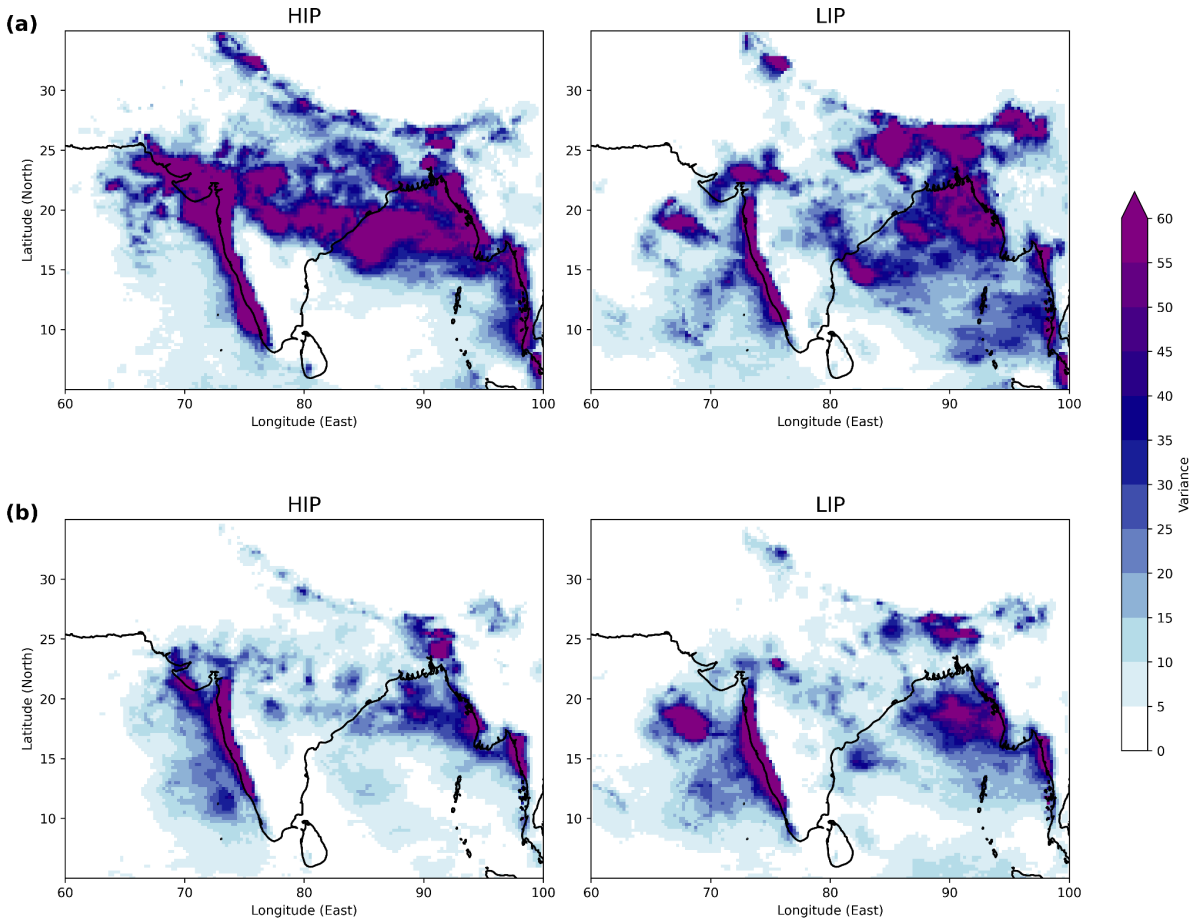
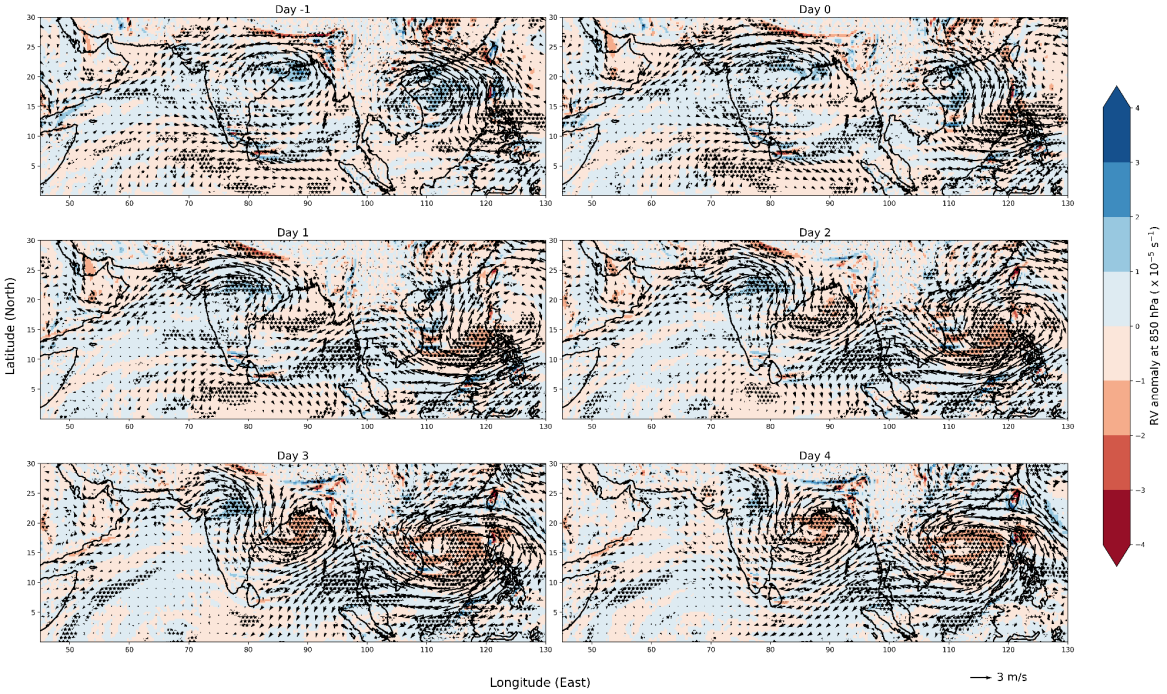
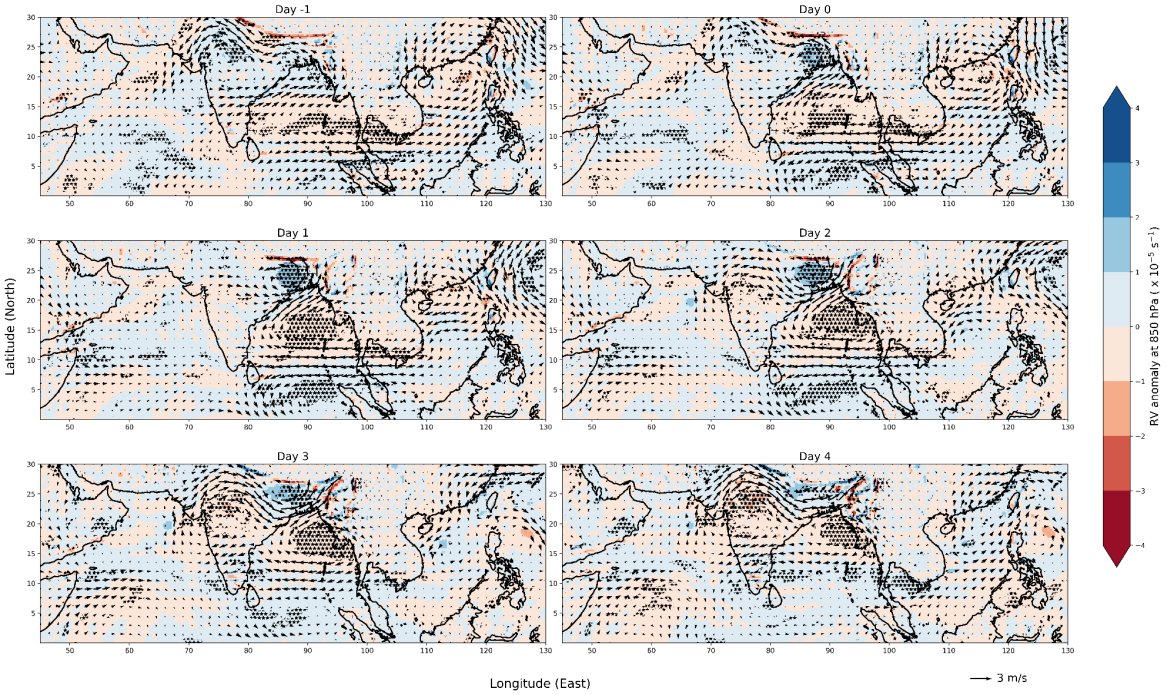


Figure 10: Variance plot for (a) 10-20 days bandpass filtered precipitation anomaly as computed using HIP (left panel) and LIP (right panel) events. In (b), same as (a), but for 30-60 days bandpass filtered precipitation anomaly. Units are in $mm^2\ day^{-2}$.



741

742 **Figure 11:** Time-lagged (from Day -1 to Day 4) plot of 10-20 days bandpass filtered anomalies
743 of ζ(x10^{-5} s^{-1}) and wind vectors (m s^{-1}) at 850 hPa level, as composited for HIP MD events.
744 Day 0 is the landfall day of each MD. In all the panels, the anomalies that are above 90%
745 confidence levels are indicated by asterisk (*).



746

747 **Figure 12:** Time-lag composite plot, similar to Figure 12, but for LIP MD events.